2 Delay and discrete growth models (Murray Ch. 1,2)

Lecture 1 introduced the continuous logistic growth model and some variants thereof (harvesting and spruce budworm model). The logistic growth model agrees well with observations for simple organisms (bacteria, yeast,...) in lab environments. For species with more complex life cycles the logistic growth model often gives a qualitative agreement but fails to describe the quantitative behaviour. In particular, an initial logistic growth is often followed by large persistent fluctuations. These can be caused by time delays due to for example finite time to become fertile and finite time of gestation (time to evolve from fetus to birth). Such time delays can be modeled using a delay model.

2.1 Delay models (M1.3–1.4)

Introduce a single delay time scale $T \geq 0$

$$\dot{N}(t) = f(N(t), N(t-T)) \,.$$

This is an example of a delay differential equation.

One example is the following extension to the logistic model (Hutchinson's equation):

$$\dot{N}(t) = rN(t)\left(1 - \frac{N(t-T)}{K}\right) , \tag{1}$$

complemented with initial condition $N(t)$ for all $-T \leq t \leq 0$. A Mathematica app for comparison of logistic growth with and without time delays is linked on the course page. Numerical solutions of Eq. (1) often show oscillatory behaviour. This is in contrast to systems without delay; an equation on the form $\dot{N} = f(N)$ cannot exhibit oscillatory dynamics (at each value of N the dynamics $\dot{N}$ always moves in the direction $f(N)$).

Linear stability analysis Introduce dimensionless variables in Eq. (1), $\tau = rt$ and $u(\tau) = N(t)/K$, and let $D = rT$ to obtain

$$\frac{\mathrm{d}}{\mathrm{d}\tau}u(\tau) = \frac{1}{rK}\frac{\mathrm{d}}{\mathrm{d}t}N(t) = u(\tau)[1 - u(\tau - D)].$$

We have two steady states $u^* = 0$ and $u^* = 1$. Write $u(\tau) = u^* + \eta(\tau)$ where $\eta(\tau)$ is small at all τ considered. Expand dynamics to first order in η:

$$\begin{aligned} &\frac{\mathrm{d}u^*}{\mathrm{d}\tau} + \frac{\mathrm{d}\eta}{\mathrm{d}\tau} = (u^* + \eta(\tau))[1 - u^* - \eta(\tau - D)] \\ &\Rightarrow \quad \frac{\mathrm{d}\eta}{\mathrm{d}\tau} \approx u^*[1 - u^*] - u^*\eta(\tau - D) + \eta(\tau)[1 - u^*]\,. \end{aligned}$$

Case $u^* = 0$:

$$\frac{\mathrm{d}\eta}{\mathrm{d}\tau}(\tau) = \eta(\tau)\,,$$

small perturbations η grow exponentially with τ. $u^* = 0$ is unstable and not of interest here.
Case $u^* = 1$:

$$\frac{\mathrm{d}\eta}{\mathrm{d}\tau}(\tau) = -\eta(\tau - D)\,.$$

Search solution on the form

$$\eta(\tau) = Ae^{\lambda\tau}\,, \text{ with complex } \lambda = \lambda' + \mathrm{i}\lambda''.$$

Inserting into the equation for η above gives

$$\lambda A e^{\lambda\tau} = -Ae^{\lambda(\tau - D)} \quad \Rightarrow \quad \lambda = -e^{-\lambda D}$$

$$\text{Real part: } \lambda' = -e^{-\lambda' D}\cos(\lambda'' D)$$

$$\text{Imaginary part: } \lambda'' = +e^{-\lambda' D}\sin(\lambda'' D)$$

These equations for λ' and λ'' have an infinite amount of solutions for any positive value of the delay D:

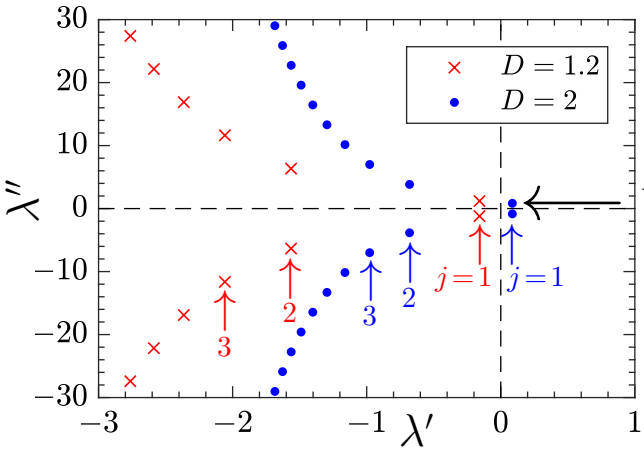

Unstable roots (with $\lambda' > 0$)

Solutions come in complex conjugate pairs $\lambda_j = \lambda'_j \pm \lambda''_j$, ordered such that $\lambda'_1 > \lambda'_2 > \ldots$ and $j = 1, \ldots, \infty$. The general solution is a superposition of the solutions corresponding to all conjugate pairs:

$$\eta(\tau) = \sum_j \left[\tilde{A}_j e^{(\lambda'_j + \mathrm{i}\lambda''_j)\tau} + \tilde{B}_j e^{(\lambda'_j - \mathrm{i}\lambda''_j)\tau} \right].$$

Choosing complex coefficients $\tilde{A}_j$ and $\tilde{B}_j$ to make $\eta(t)$ real, the solution can be written in terms of real coefficients A_j and B_j:

$$\eta(\tau) = \sum_j e^{\lambda'_j \tau} \left[A_j \cos(\lambda''_j \tau) + B_j \sin(\lambda''_j \tau) \right],$$

with A_j and B_j determined by initial condition $\eta(\tau)$ for $-D \leq \tau \leq 0$. For a random perturbation, all A_j and B_j are non-zero. It follows that if any of the real parts λ'_j is positive, a small initial random perturbation grows exponentially with time: the steady state is unstable.

Plot the real and negative imaginary part of the solution λ_1 with largest real part, λ'_1, as a function of D:

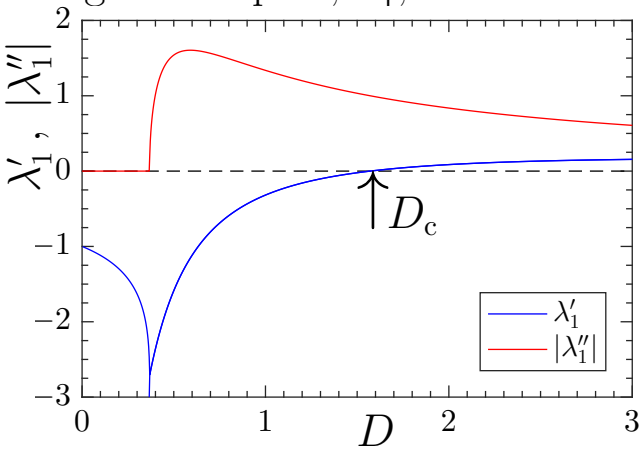

Special values

D	λ'_1	λ''_1
0	-1	0
$1/e \approx 0.37$	$-e \approx -2.72$	0
$\pi/2$	0	± 1

Inserting $\lambda_1' = 0$ in the equations for λ' and λ'' above gives simple roots $\lambda_1'' = \pm 1$ at $D_c = \pi/2$. For $0 < D < D_c$ all roots have negative real parts, $\lambda_j' < 0$ and the solution is stable: small perturbations η from the fixed point decay with time. For $D > D_c$ at least one unstable root with $\lambda_j' > 0$ exist. The system makes a qualitative transition (bifurcation) from stable to unstable at the bifurcation point $D_c = \pi/2$ where the maximal solution λ_1' becomes positive.

In conclusion, linear stability analysis predicts growing oscillations around the steady state $u^* = 1$ if the delay is large enough, $D > D_c$. This is generic, time delays typically destabilize the dynamics.

If $D > D_c$, the solution to Hutchinson's equation (1) approaches a stable limit cycle if plotted in $(N(t), N(t-T))$ space ('delay embedding'). Possible long-term dynamics in (bounded) delay models are:

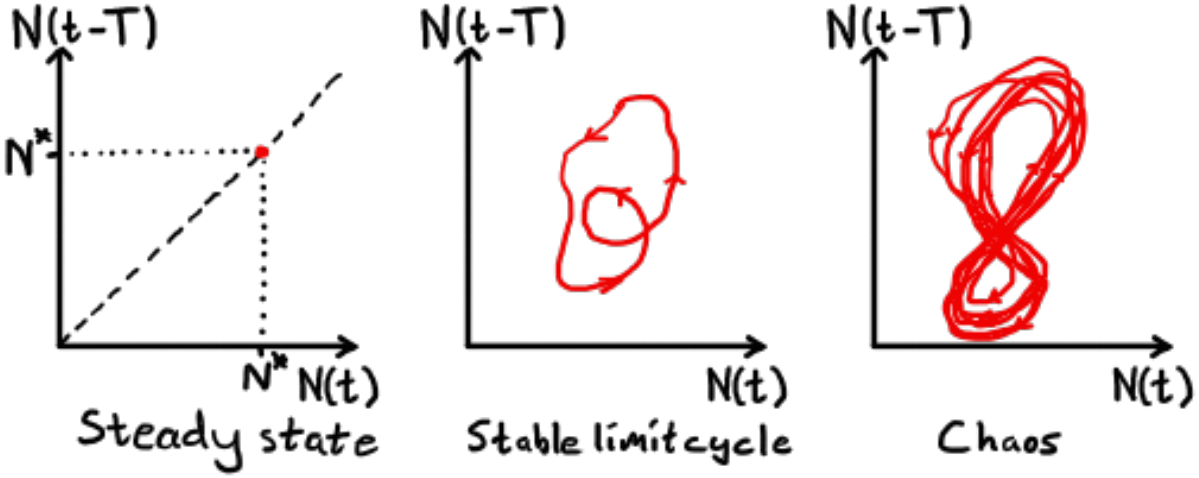

Delay models other than the Hutchinson equation (1), may show chaotic behaviour (infinitely long aperiodic attractor). One example being formation of blood cell elements in the body, Murray 1.5.

2.2 Discrete models (Murray Chapter 2)

As argued in Lecture 1, the population of non-overlapping generations can be modelled as a discrete dynamical system. This is an example of an inherently discrete dynamical system.

Discrete systems can also be obtained from continuous ones:

- **Stroboscopic map** Obtain discrete dynamics by strobing continuous flow at a sequence of times.

- **Using surface of section** Consider an n-dimensional continuous system and form an $n-1$-dimensional surface of section Γ. Construct an orbit from all crossings of a trajectory with Γ (Poincaré map from $\boldsymbol{x}_\tau$ to $\boldsymbol{x}_{\tau+1}$). Example for $n=3$:

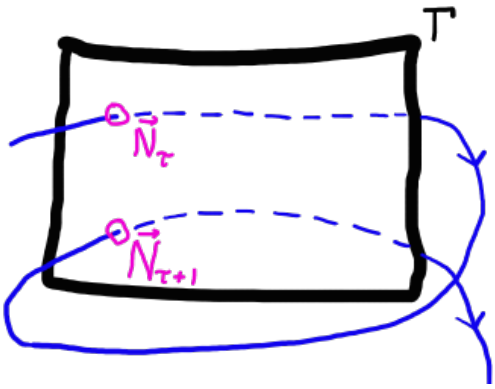

Surface of sections are used to visualise 3D (or 4D) dynamics in 2 (or 3) dimensions, or to visualize and identify periodic motion.

- **Time discretisation** of continuous system $\dot{N} = f(N)$ to for example implement a continuous model on a computer. Get

$$N(t+\delta t) \approx N(t) + \delta t f[N(t)]\,.$$

In terms of $\tau = t/\delta t$ we obtain a discrete dynamical system

$$N_{\tau+1} = \underbrace{N_\tau + \delta t f[N_\tau]}_{F(N_\tau)}\,. \tag{2}$$

Note that all continuous dynamical systems can be mapped on discrete dynamical systems, but the opposite is not true: not all discrete systems corresponds to a discretization of a continuous system.

2.3 Discrete dynamics (M2.1,2.2)

Consider the system

$$N_{\tau+1} = F(N_\tau)$$

with some map on the form $F = N_\tau + \Delta N_\tau$ that preserves $N_\tau \geq 0$.

What are reasonable shapes of the map F for a growth model? For small population sizes we assume linear growth $F \sim (1+r)N$. Due to self-regulation when the system becomes overcrowded (finite carrying capacity), we expect F to reach some maximum and then decay for large population sizes:

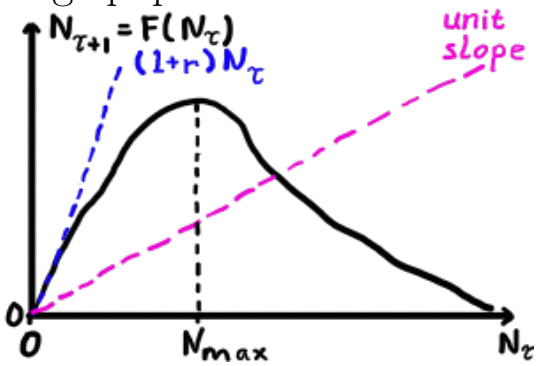

Note that the population increases if $N_{\tau+1} = F(N_\tau)$ is larger than N_τ. Graphically this translates into being in a region where $F(N_\tau)$ lies above the line of unit slope, $F(N_\tau) = N_\tau$.
Similarly the population decreases if $F(N_\tau)$ lies below $F(N_\tau) = N_\tau$. Points where $F(N_\tau)$ cross $F(N_\tau) = N_\tau$ are fixed points (steady states). Applying the map on these points do not change the population. In growth models we often have a fixed point at $N_\tau = 0$ that can be either stable (attracting) or unstable (repelling).

The dynamics of one-dimensional maps are often visualized using cobweb plots (left panel):

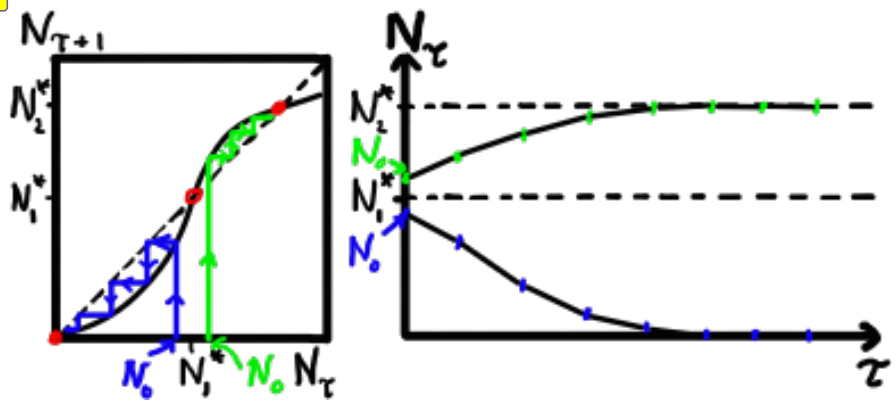

The dynamics starting at two initial conditions (blue|green) are shown.

1. From a value N_τ, move vertically to $F(N_\tau)$.
2. Move horizontally to the line $F(N) = N$. The new coordinate is $(F(N_\tau), F(N_\tau)) = (N_{\tau+1}, N_{\tau+1})$, i.e. we have found the position of $N_{\tau+1}$ on the N_τ-axis.
3. Repeat step 1 from $N_{\tau+1}$

This procedure constructs the orbit of the map (right panel above). For the case illustrated there are three fixed points: two stable at $N^* = 0$ and N_2^* and one unstable at N_1^*.

Depending on the shape of F the dynamics in the vicinity of a fixed point N^* changes:

$F'(N^*) < -1$

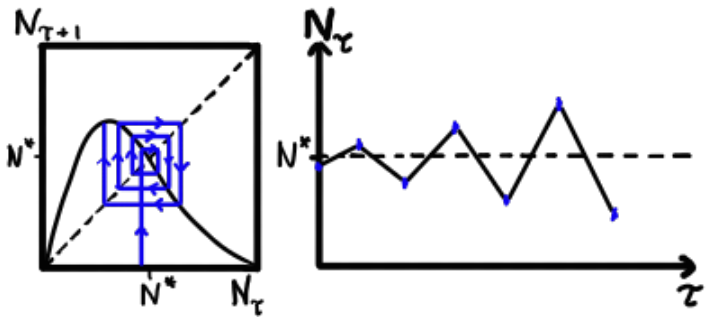

$-1 < F'(N^*) < 0$

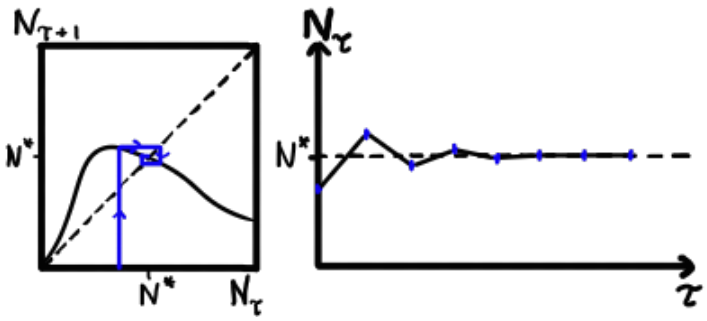

$0 < F'(N^*) < 1$

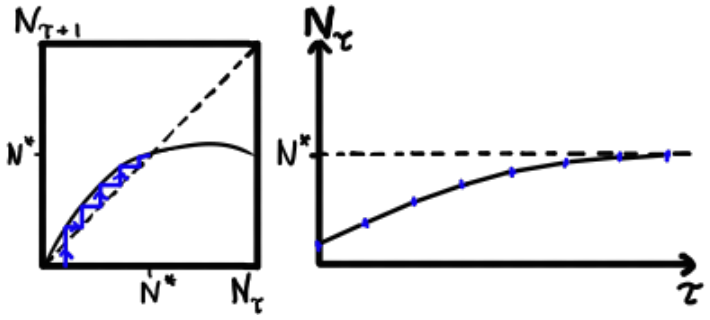

$1 < F'(N^*)$

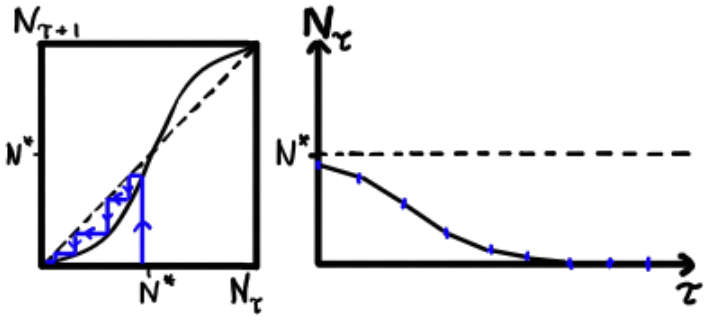

We have four distinct cases depending on the 'eigenvalue' $\Lambda \equiv F'(N^*)$:

Unstable oscillations	Stable oscillations	Stable no oscillations	Unstable no oscillations

-1 0 1 $\Lambda \equiv F'(N^*)$

Compare with the fixed points of a continuous dynamical system: stable if $f'(N^*) < 0$ and unstable if $f'(N^*) > 0$, oscillations are not possible in the continuous system because trajectories cannot intersect.

The global dynamics of a discrete one-dimensional system can be chaotic if all fixed points are unstable and if the dynamics is bounded:

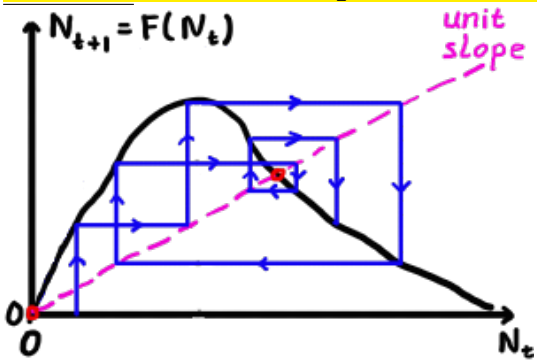

2.4 Bifurcations (M2.2,2.4)

Growth models exhibit control parameter such as the growth rate r. As the parameters change, the system may undergo bifurcations where fixed points change stability. Bifurcations occur as the eigenvalue $\Lambda = F'(N^*)$ passes through $+1$ or -1 upon variation of the control parameters. The following are examples of bifurcations with $\Lambda = +1$.

Saddle-node bifurcation (called 'tangent bifurcation' in Murray):

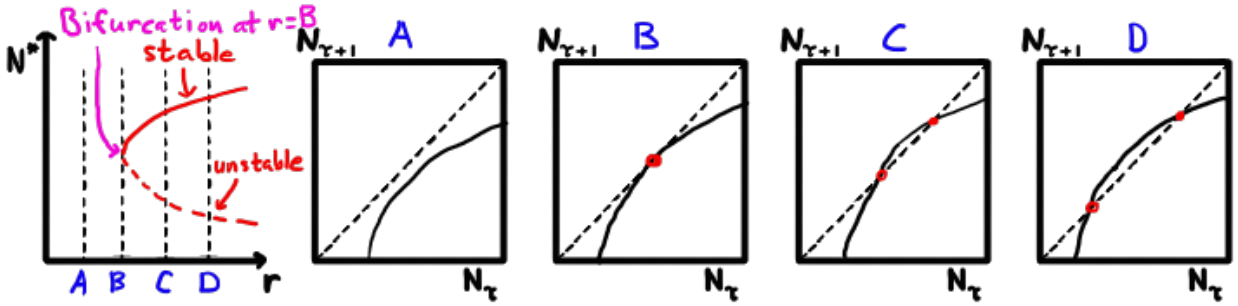

Supercritical pitchfork bifurcation

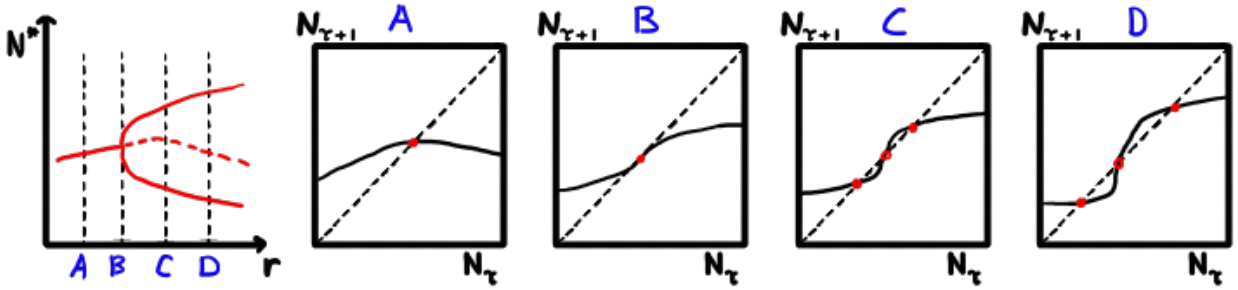

Subcritical pitchfork bifurcation

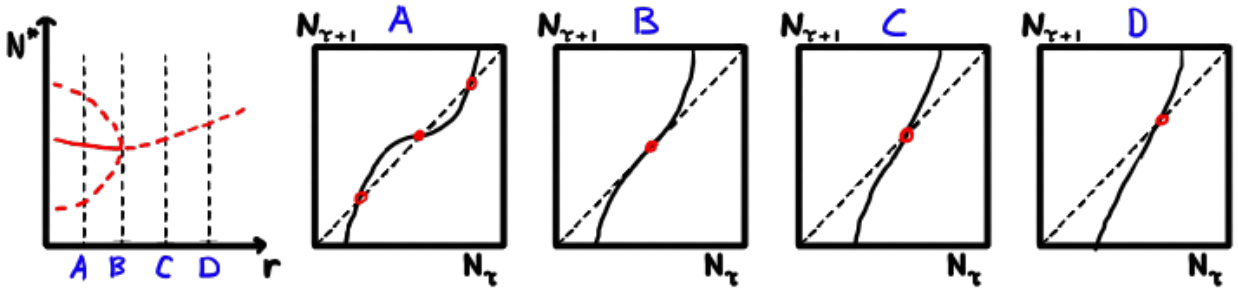

Transcritical bifurcation Stability changes as two fixed points 'move through each other'

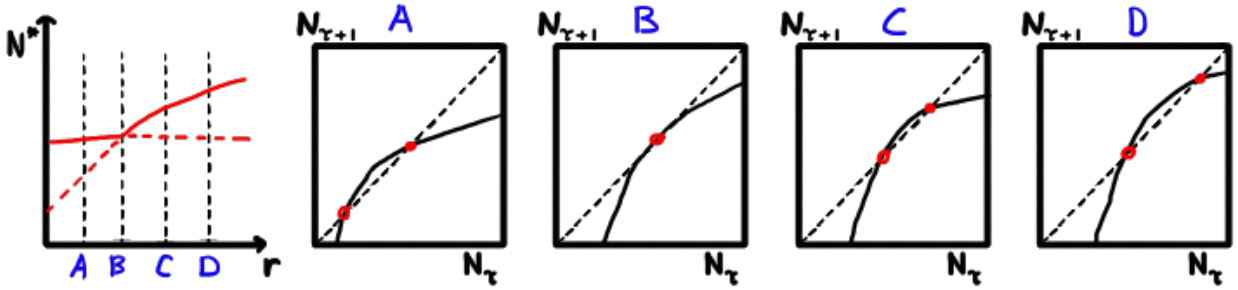

Bifurcations with $\Lambda = +1$ have counterparts in continuous dynamical systems: the time discretization (2): $F(N_\tau) = N_\tau + \delta t f(N_\tau)$ gives $F'(N_\tau^*) = 1 + \delta t f'(N_\tau^*)$. Thus, as the stability exponent $\lambda = f'(N_\tau^*)$ passes zero, the eigenvalue $\Lambda = F'(N_\tau^*)$ passes $+1$.

In addition to the examples above, discrete systems may also have bifurcations as Λ passes -1, for example period-doubling bifurcations where a stable fixed point transforms into an attracting periodic cycle.

Period-doubling bifurcation Assume map $N_{\tau+1} = F(N_\tau)$ has an isolated fixed point $N_{(1)}^*$ and that $\Lambda = F'(N_{(1)}^*)$ passes through -1 at bifurcation point $r = B$

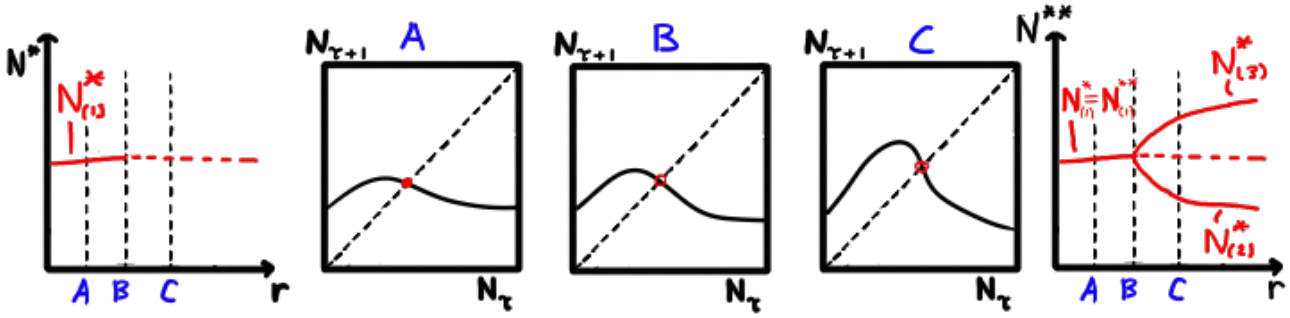

Denote fixed points of the second iterate of the map by $N_{(i)}^{**}$. One fixed

point is $N^{**}_{(1)} = N^{*}_{(1)}$ because $F(F(N^{*}_{(1)})) = N^{*}_{(1)}$. It has eigenvalue

$$\frac{\mathrm{d}}{\mathrm{d}N}F(F(N))|_{N=N^{**}_{(1)}} = F'(F(N^{*}_{(1)}))F'(N^{*}_{(1)}) = \Lambda^2 \,.$$

Thus, at $r = B$ the eigenvalue of the second iterate passes $\Lambda^2 = (-1)^2 = +1$ and the second iterate (typically) undergoes a pitchfork bifurcation, forming two new stable fixed points $N^{**}_{(2)}$ and $N^{**}_{(3)}$ (illustrated in right-most panel above). These form an alternating solution to the original map: $N_\tau = N^{**}_{(2)}, N^{**}_{(3)}, N^{**}_{(2)}, N^{**}_{(3)}, \ldots$, i.e. a stable period-two cycle of the original map. Period-doubling bifurcations are frequent in the logistic map and other discrete growth models.

2.5 Example: Logistic map (M2.3)

The logistic map is a discrete system having the same form of the rate of change of population ΔN as the logistic equation from Lecture 1

$$N_{\tau+1} = N_\tau + rN_\tau\left(1 - \frac{N_\tau}{K}\right) \,.$$

2.5.1 Comparison to logistic equation

The following figure shows a numerical comparison of continuous and discrete logistic models for two growth rates ($N_0 = 10$, $K = 750$):

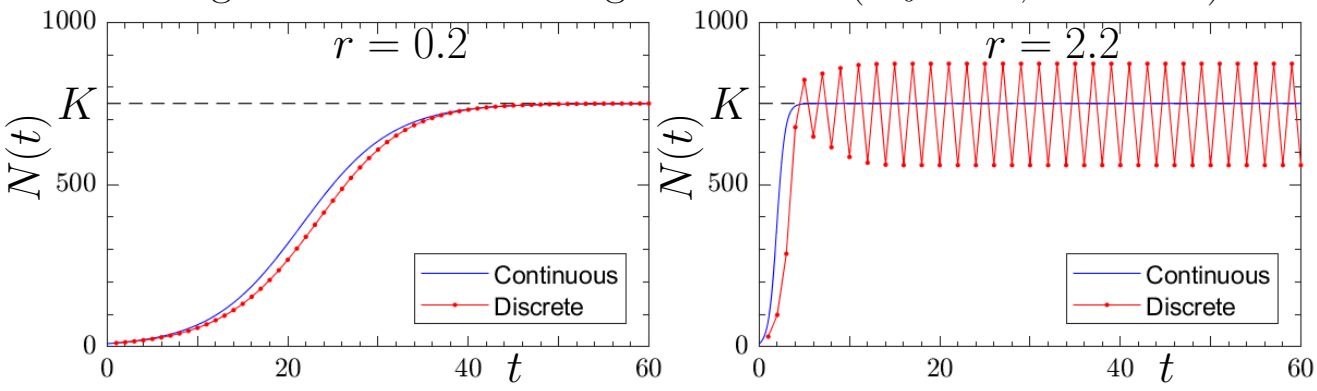

The two models agree for small values of r. For larger values of r there can be significant difference. In the example shown, the discrete model shows oscillations with period 2. A detailed analysis (below) shows that the discrete map has a fixed point at $N^* = K$, but that this fixed

point has undergone a period-doubling bifurcation at $r = 2$ and the dynamics is therefore attracted to a stable period-two cycle.

In conclusion, the inherent time delay of discrete models often give rise to unsteady or oscillatory behaviour similar to the effect of delay in continuous models above.

2.5.2 Analysis[1]

Introduce a dimensionless population size $u_\tau \equiv N_\tau r/(K(r+1))$ and define $\rho \equiv r + 1$ in the logistic map:

$$u_{\tau+1} = \rho u_\tau \left(1 - u_\tau\right) . \tag{3}$$

Assume $0 < u_0 < 1$ and $0 < \rho \leq 4$ (population size may become negative if $\rho > 4$). The dimensionless logistic map (3) has two fixed points with corresponding eigenvalues Λ:

$$u^*_{(1)} = 0 \qquad \Lambda = F'(0) = \rho$$
$$u^*_{(2)} = 1 - \frac{1}{\rho} \qquad \Lambda = F'\left(1 - \frac{1}{\rho}\right) = 2 - \rho\,.$$

For $0 < \rho < 1$, $u^*_{(1)} = 0$ is stable and the first bifurcation (transcritical) happens at $\rho = 1$ where $u^*_{(1)} = 0$ becomes unstable.

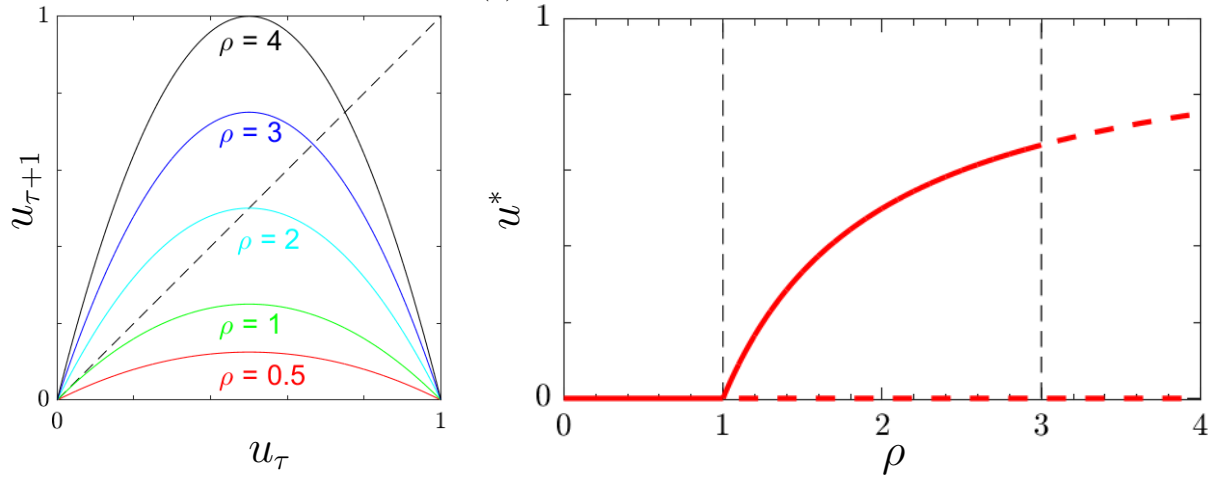

[1]The details in this subsection are not part of the course content and can be skipped. They illustrate mathematically how the period-doubling cascade forms for the logistic map. Note that Section 2.5.3 on the qualitative features of the period-doubling cascade belongs to the course content.

For $1 < \rho < 3$, $u^*_{(1)} = 0$ is unstable and $u^*_{(2)}$ is stable.
$\Lambda = -1$ for $u^*_{(2)}$ when $\rho = 3$ and the system has no stable fixed points when $\rho > \rho_1 = 3$. In order to understand the bifurcation, we must consider higher-order iterates of the map as follows. In general the points on an orbit are obtained by successive application of the map:

$$\begin{aligned} u_1 &= F(u_0) \\ u_2 &= F(F(u_0)) \equiv F^2(u_0) \\ &\vdots \\ u_\tau &= F^\tau(u_0)\,. \end{aligned}$$

For the second iterate of F:

$$u_{\tau+2} = F^2(u_\tau) = \rho\big[\underbrace{\rho u_\tau\,(1-u_\tau)}_{u_{\tau+1}}\big]\big(1 - \underbrace{\rho u_\tau\,(1-u_\tau)}_{u_{\tau+1}}\big) \qquad (4)$$

Denote fixed points of the map F^2 by u^{**}. When ρ passes through 3, $F^2(u_\tau)$ undergoes a pitchfork bifurcation:

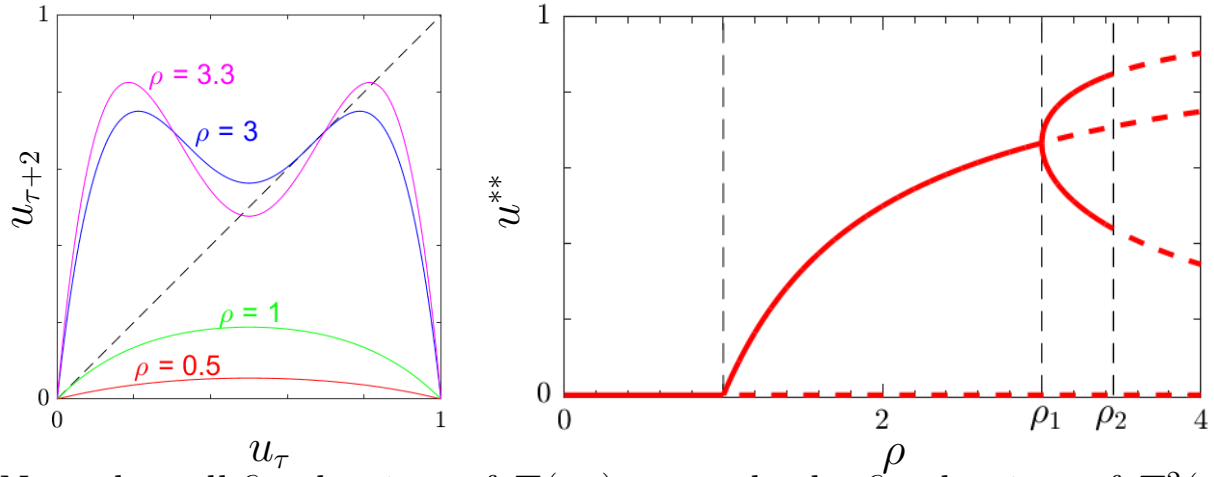

Note that all fixed points of $F(u_\tau)$ must also be fixed points of $F^2(u_\tau)$, $u^{**}_{(1)} \equiv u^*_{(1)} = 0$ and $u^{**}_{(2)} \equiv u^*_{(2)} = 1 - \rho^{-1}$, but the eigenvalue may be different. As we saw above, when ρ passes 3, the eigenvalue

$$\Lambda \equiv F'(u^*_{(2)}) = 2 - \rho$$

decreases through -1 and $u^*_{(2)}$ becomes unstable. At the same time

$$F^{2\prime}(u^{**}_{(2)}) = \frac{\partial}{\partial u} F(F(u))\bigg|_{u^*_{(2)}} = F'(\underbrace{F(u^*_{(2)})}_{u^*_{(2)}})F'(u^*_{(2)}) = [F'(u^*_{(2)})]^2 = \Lambda^2$$

increases through $\Lambda^2 = (-1)^2 = +1$ and two new stable fixed points $u^{**}_{(3),(4)}$ of $F^2(u_\tau)$ are created in a pitchfork bifurcation:

$$u^{**}_{(3),(4)} = \frac{\rho + 1 \pm \sqrt{(\rho - 3)(\rho + 1)}}{2\rho} \,.$$

These are stable (if ρ is not too large) and satisfies

$$F^2(u^{**}_{(3)}) = u^{**}_{(3)} \text{ and } F^2(u^{**}_{(4)}) = u^{**}_{(4)}$$

but they are not fixed points of F:

$$F(u^{**}_{(3)}) \neq u^{**}_{(3)} \text{ and } F(u^{**}_{(4)}) \neq u^{**}_{(4)} \,.$$

It follows that $F(u^{**}_{(3)}) = u^{**}_{(4)}$ and $F(u^{**}_{(4)}) = u^{**}_{(3)}$, i.e. the system approaches a stable period-two cycle $u^{**}_{(3)}$, $u^{**}_{(4)}$, $u^{**}_{(3)}$, $u^{**}_{(4)}$, ...
In conclusion: exactly when the period-one fixed point $u^{*}_{(2)} = 1 - \rho^{-1}$ becomes unstable a new period-two cycle is created (period-doubling bifurcation), c.f. Section 2.5.1.

Note that the eigenvalues of $u^{**}_{(3),(4)}$ must be equal because they form a cycle for the original map:

$$\Lambda_3 \equiv F^{2\prime}(u^{**}_{(3)}) = \frac{\partial}{\partial u} F(F(u))\bigg|_{u^{**}_{(3)}} = F'(\underbrace{F(u^{**}_{(3)})}_{u^{**}_{(4)}}) F'(u^{**}_{(3)}) = F'(u^{**}_{(3)}) F'(u^{**}_{(4)}) \,.$$

In the same way

$$\Lambda_4 \equiv F^{2\prime}(u^{**}_{(4)}) = F'(u^{**}_{(3)}) F'(u^{**}_{(4)}) \,.$$

As ρ passes $\rho_2 \approx 3.45$ the eigenvalues $\Lambda_3 = \Lambda_4$ simultaneously pass -1 and another period-doubling bifurcation occurs (four new stable fixed points are formed in the map F^4), creating an attracting period-four cycle in the original map (stable up to $\rho_3 \approx 3.54$):

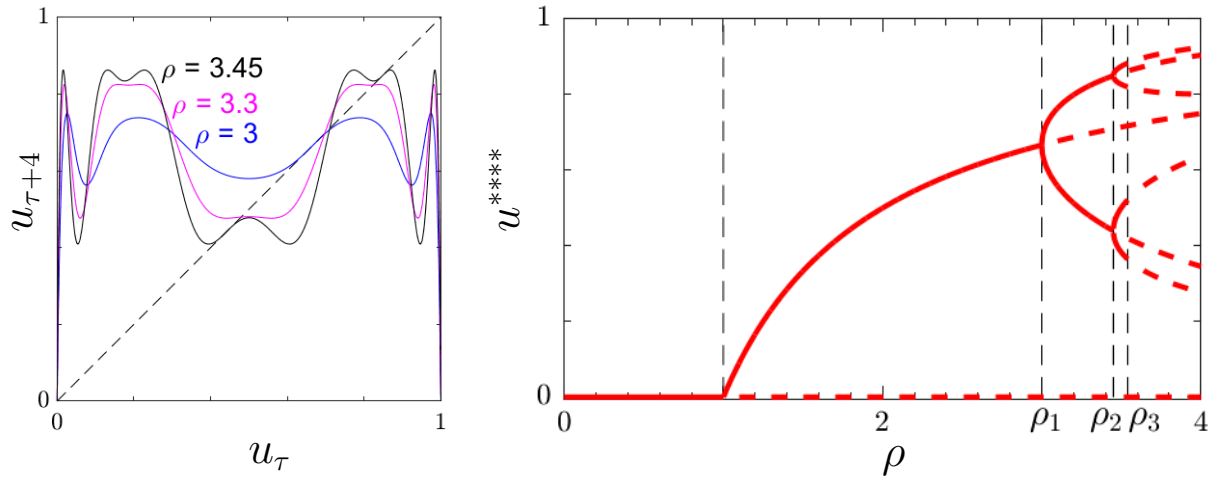

2.5.3 Period-doubling cascade

Subsequent period doubling bifurcations give rise to a period-doubling cascade, consisting of bifurcation values ρ_i, $i = 1, 2, \ldots$, where period 2^i-cycles are formed. The stable attracting cycle is obtained by plotting large-time iterates of the map:

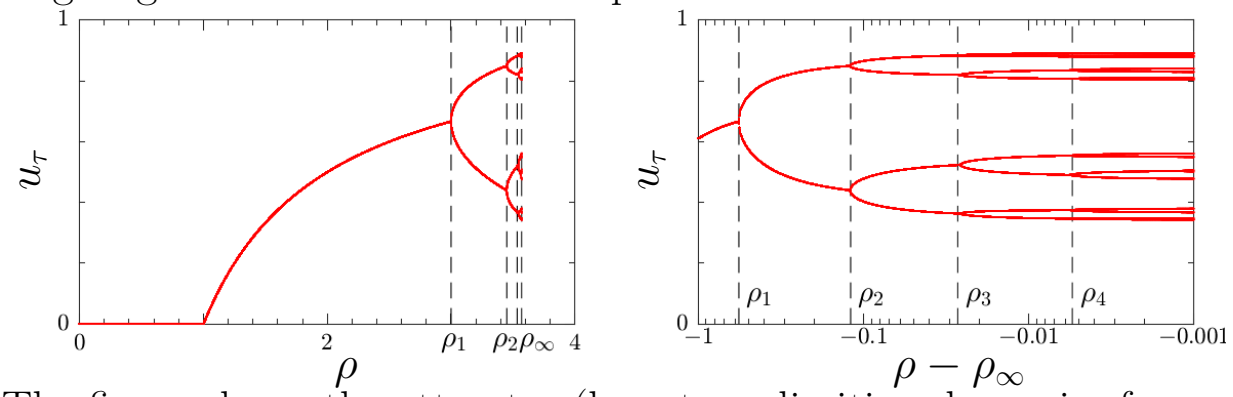

The figure shows the attractor (long term limiting dynamics for most initial conditions) of the logistic map for different values of ρ on a linear (left) and logarithmic (right) scale. Unstable fixed points and cycles are only visited for a discrete set of isolated initial conditions and are not shown.

Feigenbaum (1978) showed that distances between pairs of subsequent bifurcations approach a universal limit

$$\frac{\rho_i - \rho_{i-1}}{\rho_{i+1} - \rho_i} \to 4.669\cdots \equiv \delta \tag{5}$$

as $i \to \infty$. Eq. (5) implies that subsequent bifurcations come closer and closer as $i \to \infty$, and there exists a finite value where the period

becomes infinite, $\rho_\infty \equiv \lim_{i\to\infty} \rho_i$. For the logistic map $\rho_\infty \approx 3.56995$. Solving Eq. (5) for ρ_i shows that $|\rho_\infty - \rho_i| \sim \delta^{-i}$ for large i, i.e. steps between subsequent bifurcations become uniformly distributed when plotted on a log-scale (see right panel above).

Extending the range up to $\rho = 4$:

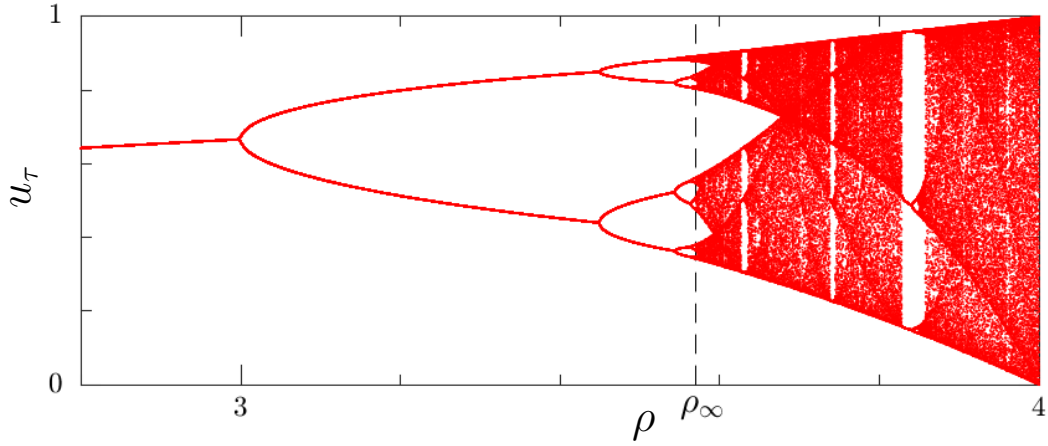

reveals complicated dynamics: when $\rho > \rho_\infty$ attractors are either periodic cycles or aperiodic attractors. For $\rho = 4$ the aperiodic attractor fills the entire interval. For other values of ρ the aperiodic attractor splits to fill a number of smaller intervals, e.g. 2 bands at $\rho \approx 3.63$. Such aperiodic attractors are characterized by

1. Apparently irregular orbit
2. Re-appearance of the full pattern in small windows (fractal structure):

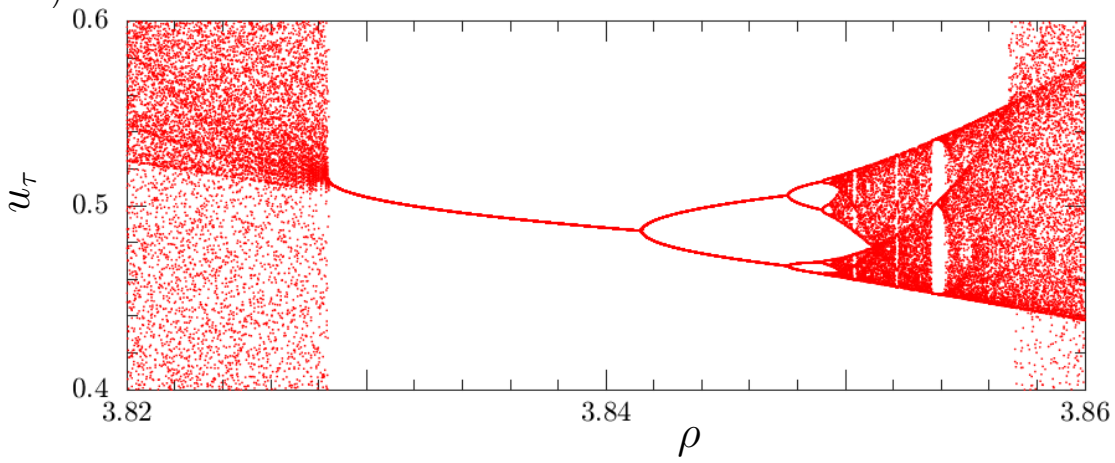

3. Enhanced sensitivity to changes in initial condition u_0

This behaviour is called deterministic chaos: the dynamics appears irregular despite being deterministic. More precisely: Deterministic

chaos describes aperiodic, bounded deterministic dynamics with enhanced sensitivity to small changes of initial conditions.

The period-doubling cascade leading to chaotic behavior shown here is a common route to chaos. It shows several universal features, for example $\delta = 4.669\ldots$ takes the same value for many systems.

2.6 Higher dimensional discrete maps[2]

The graphical analysis for the one-dimensional discrete systems of the previous sections is here complemented with an analytical formulation, valid also for higher dimensions. Consider a general map

$$\boldsymbol{x}_{\tau+1} = \boldsymbol{F}(\boldsymbol{x}_\tau)\,.$$

What happens to a small perturbation $\boldsymbol{x}^* + \delta\boldsymbol{x}$ after many iterations?

Let $\boldsymbol{F}^n(\boldsymbol{x}) \equiv \boldsymbol{F}(\boldsymbol{F}(\cdots \boldsymbol{F}(\boldsymbol{x})))$ denote a map applied n times. First evaluate the derivative of $\boldsymbol{F}^n(\boldsymbol{x})$ at a fixed point $\boldsymbol{x}^*$. First $d = 1$:

$$\begin{aligned}\left.\frac{\partial}{\partial x}F^n(x)\right|_{x=x^*} &= \left.\frac{\partial}{\partial x}F(F^{n-1}(x))\right|_{x=x^*} \\ &= \frac{\partial F}{\partial x}(\underbrace{F^{n-1}(x^*)}_{x^*})\left.\frac{\partial}{\partial x}F^{n-1}(x)\right|_{x=x^*} = \left[\frac{\partial F}{\partial x}(x^*)\right]^n\end{aligned}$$

General dimension

$$\left.\frac{\partial}{\partial \boldsymbol{x}}\boldsymbol{F}^n(\boldsymbol{x})\right|_{\boldsymbol{x}=\boldsymbol{x}^*} = [\mathbb{J}(\boldsymbol{x}^*)]^n\,,$$

with $\mathbb{J}$ the gradient matrix $\partial\boldsymbol{F}/\partial\boldsymbol{x}$.

$\Rightarrow$ to first order we have

$$\boldsymbol{F}^n(\boldsymbol{x}^* + \delta\boldsymbol{x}) \approx \underbrace{\boldsymbol{F}^n(\boldsymbol{x}^*)}_{\boldsymbol{x}^*} + \underbrace{\frac{\partial}{\partial\boldsymbol{x}}\boldsymbol{F}^n(\boldsymbol{x}^*)}_{[\mathbb{J}(\boldsymbol{x}^*)]^n}\delta\boldsymbol{x} = \boldsymbol{x}^* + [\mathbb{J}(\boldsymbol{x}^*)]^n\delta\boldsymbol{x}$$

[2]Higher dimensional discrete maps is not part of the course content, but as a reference it could be good to have a hint of the theory which is outlined in this section (in particular the comparison between maps and flows on the last page could be relevant).

Let Λ_i and $\boldsymbol{e}_i$ be eigenvalues and eigendirections of $\mathbb{J}(\boldsymbol{x}^*)$:

$$\mathbb{J}(\boldsymbol{x}^*)\boldsymbol{e}_i = \Lambda_i \boldsymbol{e}_i \,.$$

It follows

$$[\mathbb{J}(\boldsymbol{x}^*)]^n \boldsymbol{e}_i = \Lambda_i^n \boldsymbol{e}_i \,.$$

By decomposition of $\delta\boldsymbol{x}$ in terms of $\boldsymbol{e}_i$, i.e. $\delta\boldsymbol{x} = \sum_i a_i \boldsymbol{e}_i$ it follows

$$[\mathbb{J}(\boldsymbol{x}^*)]^n \delta\boldsymbol{x} = \sum_i a_i \Lambda_i^n \boldsymbol{e}_i \,.$$

- Eigendirections with $|\Lambda_i| < 1$ contracting for large n
- Eigendirections with $|\Lambda_i| > 1$ expanding for large n
- Eigendirections with $|\Lambda_i| = 1$ marginal for large n

The fixed point is stable if all $|\Lambda_i| < 1$.
If any $|\Lambda_i| > 1$ the fixed point is unstable.

2.6.1 p-cycles

As found above, discrete maps may show periodic motion. The fixed points of a map applied twice: $N_{\tau+2} = F(F(N_\tau))$ are 2-cycles i.e. the orbit is $N_0, N_1, N_0, \ldots$.
Any fixed point of the map satisfies $F^p(N^*) = N^*$ for any p.
Fixed points of $N_{\tau+p} = F^p(N_t)$ are cycles of period p.
The shortest cycle of N_τ is called prime cycle (p-cycle)

Summary: Comparison maps and flows -

	Flow $\boldsymbol{f}$	Map $\boldsymbol{F}$
System	Continuous ODE	Discrete difference equations
	$\dot{\boldsymbol{x}} = \boldsymbol{f}(\boldsymbol{x})$	$\boldsymbol{x}_{\tau+1} = \boldsymbol{F}(\boldsymbol{x}_\tau)$
Solution	Trajectory $\boldsymbol{x}(t)$	Orbit $\{\boldsymbol{x}_0, \boldsymbol{x}_1, \ldots\}$
Periodic solution	Closed orbit $\boldsymbol{x}(t) = \boldsymbol{x}(t+T)$	Cycle $\boldsymbol{x}_{\tau+T} = \boldsymbol{x}_\tau$
		(fixed point of $\boldsymbol{F}^T(\boldsymbol{x}_\tau)$)
Fixed point cond.	$\boldsymbol{f}(\boldsymbol{x}^*) = \boldsymbol{0}$	$\boldsymbol{F}(\boldsymbol{x}^*) = \boldsymbol{x}^*$
Chaos possible	If $d > 2$	$d = 1$ if non-invertible map
		otherwise $d > 1$
Jacobian	$J_{ij} = \partial f_i / \partial x_j$	$J_{ij} = \partial F_i / \partial x_j$
Area preserving if	$\boldsymbol{\nabla} \cdot \dot{\boldsymbol{x}} = \mathrm{tr}\mathbb{J} = 0$	$\det \mathbb{J} = 1$
Eigenvalues at fixed point	λ_i ($\mathcal{R}e[\lambda_i]$ determines stability)	Λ_i ($\lvert\Lambda_i\rvert$ determines stability)
Stable node (2D)	$\lambda_1 < \lambda_2 < 0$ and $\mathcal{I}m[\lambda_{1,2}] = 0$	$\lvert\Lambda_1\rvert < \lvert\Lambda_2\rvert < 1$ and $\mathcal{I}m[\Lambda_{1,2}] = 0$
Unstable node (2D)	$\lambda_1 > \lambda_2 > 0$ and $\mathcal{I}m[\lambda_{1,2}] = 0$	$\lvert\Lambda_1\rvert > \lvert\Lambda_2\rvert > 1$ and $\mathcal{I}m[\Lambda_{1,2}] = 0$
Saddle (unstable) (2D)	$\lambda_1 < 0 < \lambda_2$ and $\mathcal{I}m[\lambda_{1,2}] = 0$	$\lvert\Lambda_1\rvert < 1 < \lvert\Lambda_2\rvert$ and $\mathcal{I}m[\Lambda_{1,2}] = 0$
Stable spiral (2D)	$\lambda_{1,2} = \mu \pm \mathrm{i}\omega$ and $\mu < 0$	$\Lambda_{1,2} = \rho e^{\pm \mathrm{i}\theta}$ and $\rho < 1$
Unstable spiral (2D)	$\lambda_{1,2} = \mu \pm \mathrm{i}\omega$ and $\mu > 0$	$\Lambda_{1,2} = \rho e^{\pm \mathrm{i}\theta}$ and $\rho > 1$
Center (2D)	$\lambda_{1,2} = \pm \mathrm{i}\omega$	$\Lambda_{1,2} = e^{\pm \mathrm{i}\theta}$